Medical Engineering & Physics 32 (2010) 898–907

Contents lists available at ScienceDirect

Medical Engineering & Physics

journal homepage: www.elsevier.com/locate/medengphy

Numerical analysis of recurrence plots to detect effect of environmental-strength magnetic fields on human brain electrical activity

Simona Carrubba[a], Clifton Frilot II[b], Andrew L. Chesson Jr.[a], Andrew A. Marino[c,*]

[a] Department of Neurology, LSU Health Sciences Center-Shreveport, United States
[b] School of Allied Health Professions, LSU Health Sciences Center-Shreveport, United States
[c] Department of Neurology, LSU Health Sciences Center-Shreveport, P.O. Box 33932, Shreveport, LA 71130-3932, United States

ARTICLE INFO

Article history:
Received 30 December 2009
Received in revised form 15 June 2010
Accepted 19 June 2010

Keywords:
Recurrence plots
Nonlinear analysis
Magnetic field
Sensory transduction
Electroencephalogram
Time averaging

ABSTRACT

Environmental magnetic fields may activate the neuroendocrine stressor system leading to some human diseases. The stressor theory predicts that the fields can trigger changes in brain electrical activity, like known stressors. We exposed subjects to 1 and 5 μT, 60 Hz while recording electroencephalograms (EEGs) from six derivations, and used a novel method based on numerical analysis of recurrence plots computed from the signals to detect brain electrical potentials evoked by onset and/or offset of the field. The EEGs were also analyzed using linear methods (time averaging). Evoked potentials occurred in all 22 subjects (family-wise error rate less than 0.05 for each subject); the average latency was 250 ms, as expected based on earlier studies using stronger magnetic fields. Field-induced changes in brain electrical activity were not found using time averaging. Control procedures and measurements obtained from electrical phantoms reasonably excluded recording artifacts or chance as explanations for the effects. Onset and offset of magnetic fields produced immediate changes in brain electrical activity, suggesting that the fields were detected by sensory transduction, like ordinary somatic stressors.

1. Introduction

The ubiquitous presence of power-frequency electromagnetic fields (EMFs) in the general and workplace environments has prompted long-standing questions concerning whether the fields were partly responsible for brain cancer or other diseases. With few exceptions, the fields are too weak to heat tissue or directly depolarize axons, but the processes responsible for mediating the effects attributed to EMFs are not clearly established. One of us (AAM) proposed that environmental EMFs can be biological stressors [1], and that the link with disease stems from chronic stimulation of the hypothalamic-pituitary-adrenal axis [2] which results in impaired immune surveillance [3,4].

Initiation of efferent neuroendocrine signals by ordinary energetic environmental stressors such as heat, sound, light, and physical contact is preceded by afferent signals triggered by sensory transduction. The EMF stressor theory therefore entails the hypothesis that environmental fields are similarly detected by sensory transduction. If so, we would expect that environmental EMFs would be capable of inducing immediate changes in brain electrical activity, like the common stimuli.

Using recurrence-plot analysis, a phase-space-based analytical technique developed to facilitate study of nonlinear dynamical systems [5], we previously reported that exposure to magnetic fields about two orders greater than those typically found in the environment triggered onset and offset evoked potentials (EPs) with average latencies of about 250 ms [6]. Evoked potentials were not found using linear analytical techniques such as time averaging and spectral analysis, implying that the stimulus–response relationships were governed by nonlinear processes in the brain. Our present aim was to determine whether magnetic fields having strengths directly comparable to those typically found in the environment also elicited EPs. Specifically we tested the hypothesis that exposure to 1–5 μT, 60 Hz, produced nonlinear onset and/or offset EPs.

2. Methods

2.1. Subjects

Twenty-two clinically normal subjects volunteered for the study: 10 males (age range 23–61 years) and 12 females (22–58 years). The subjects were informed of the goals, methods, and general design of the investigation, but were not told exactly when or for how long the field would be applied. Written informed consent was obtained from each subject prior to participation in the study.

* Corresponding author. Tel.: +1 318 675 6180; fax: +1 318 675 6186.
E-mail address: amarino@lsuhsc.edu (A.A. Marino).

1350-4533/$ – see front matter © 2010 IPEM. Published by Elsevier Ltd. All rights reserved.
doi:10.1016/j.medengphy.2010.06.006

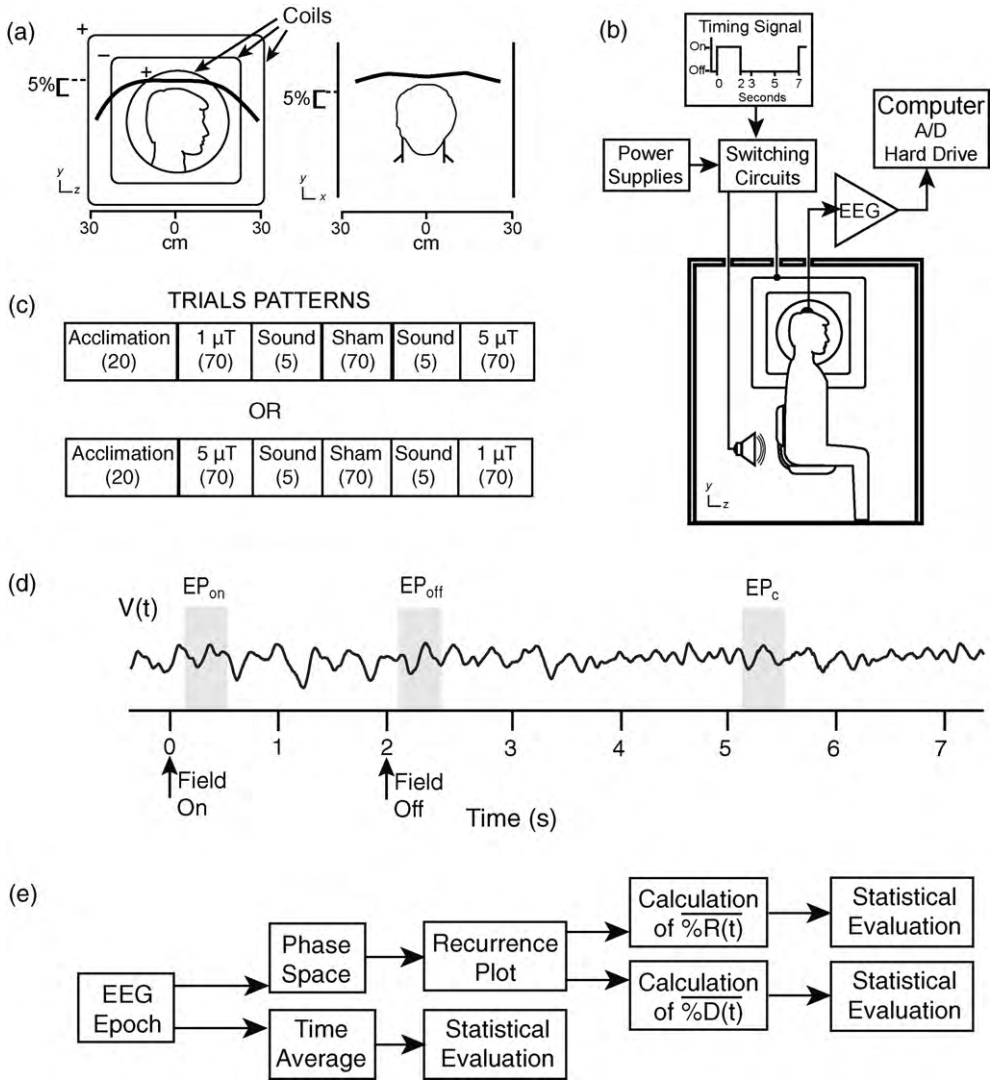

Fig. 1. Apparatus and procedure for applying magnetic fields and detecting induced changes in brain electrical activity. (a) Magnetic field generated by two sets of coils, each consisting of two square coils and one round coil; relative direction of current flow in the coils, +, −, +. The field varied less than 5% in the vicinity of the subject's head. (b) Schematic diagram of equipment for applying stimuli and recording the EEG; A/D, analog-to-digital. (c) Organization of trials in the experimental sessions; number of 7-s trials shown in parentheses. (d) Division of a trial into epochs to facilitate detection of transient and steady-state changes in the electroencephalogram ($V(t)$) induced by the magnetic field. EP_{on}, EP_{off}, EP_C, onset, offset, and control epochs, respectively, used for detection of onset and offset evoked potentials. (e) Nonlinear and linear analytical procedures for detecting changes in the EEG due to magnetic fields. $\overline{\%R}$ and $\overline{\%D}$, nonlinear quantifiers.

The review board for human research at the LSU Health Sciences Center approved all experimental procedures.

2.2. Magnetic field

Sinusoidal 60-Hz magnetic fields were generated using two sets of three coaxial, coplanar coils (Fig. 1a). Each set consisted of a circular coil (21 turns, radius of 21.6 cm), and two square coils (85 turns, 120 turns, respective side length of 48.3 and 66 cm). The coils were shielded with grounded aluminum foil to eliminate the 60–Hz electric field (<1 V/m). The coil current (801 RP, California Instruments, San Diego, CA) was turned on and off by a microcontroller. The expected field uniformity in the head region (±5%) was verified by measurement (Bartington, MAG-03, GMW, Redwood City, CA, USA).

The magnetic stimuli were applied in a dark isolation chamber to mitigate the effect of irrelevant or random ambient stimuli; the subjects sat with their eyes closed and their sagittal plane perpendicular to the field (Fig. 1b). The equipment that controlled the coils and recorded the electroencephalograms (EEGs) was located outside the chamber. The absence of both sensory cues and conscious perception of the field were verified by interviewing each subject at the end of the experimental session.

The field was presented for 2-s intervals (rise and fall times, <10 ms), with inter-stimulus intervals of 5 s (7-s trials). Each subject underwent 3 blocks of trials (70 trials/block) in which, following acclimation (approximately 2 min), magnetic fields of 1 and 5 μT (rms) were applied in the first and third block (order of presentation chosen randomly from subject to subject); an auditory stimulus (424 Hz, 65 db) was applied (2 s on and 5 s off, $N = 5$) to help maintain alertness (Fig. 1c). The data from the middle block (sham exposure) was analyzed as a negative control. The background 60-Hz magnetic field (field present when the coils were not energized) was 0.01 μT; the geomagnetic field was 60 μT, 68.4° below the horizontal (component along the direction of the applied field, 36 μT).

2.3. EEG recording

Electroencephalograms were recorded from O1, O2, C3, C4, P3, and P4 (International 10–20 system) referenced to linked ears,

using gold-plated electrodes attached to the scalp with conductive paste. Electrode impedances (measured before and after each experiment) were less than 10 kΩ in all subjects. The signals were amplified (Nihon Kohden, Irvine, CA, USA), analog-filtered to pass 0.5–35 Hz, sampled at 5 kHz using a 12-bit analog-to-digital converter (National Instruments, Austin, TX, USA), and analyzed offline. Each signal, $V(t)$, was divided into consecutive 7-s trials with field onset at $t = 0$, offset at $t = 2$ s, and an inter-stimulus period at $2 < t \leq 7$ s (Fig. 1d). Trials containing any of 10 recognized artifacts (both physiological and nonphysiological) [7] as assessed by visual inspection were discarded (<5% of all trials), and the artifact-free trials were sub-sampled at 300 Hz.

Because of faradaic induction, the onset and offset of coil currents that produced 100–200 μT resulted in spikes in $V(t)$ lasting about 10 ms; additionally, the presence of the fields induced a steady voltage that added to the physiological signal [8]. The fields used here, in contrast, produced neither spikes nor a steady component in $V(t)$; nevertheless, as in our previous studies, the 30-ms intervals following signal onset and offset ($t = 0$–30 ms, $t = 2.000$–2.030 s) were deleted from $V(t)$, after which the signal was digitally filtered to pass 0.5–35 Hz. All results were based on data from at least 50 trials.

2.4. Detection of evoked potentials

Recurrence-plot analysis (RA) was used to detect field-induced nonlinear determinism in $V(t)$; the method imposes no constraints on the stationarity or statistical characteristics of $V(t)$ [5]. The determinism was identified by analyzing time-lagged versions of $V(t)$ in a hyper-dimensional phase space [9], mapping the trajectory of the system to a two-dimensional recurrence plot [10], and quantitating the plot using specific variables [5] (see below).

More particularly, a phase space was constructed for each specific interval of interest in $V(t)$. If an interval in $V(t)$ containing N points were embedded in an M-dimensional phase space with a lag of τ points the resulting trajectory would consist of $N - \tau(M-1)$ M-dimensional vectors, from which a recurrence plot could be computed, yielding a single value of the recurrence variables. To achieve our goal of detecting transient changes in $V(t)$, we iterated this process to form time series for the recurrence variables. The first 30 points in $V(t)$ ($t = 30$–130 ms) (RA window) were embedded in a five-dimensional phase space to form a trajectory of 30–5(5–1) = 10 vectors, a corresponding recurrence plot was calculated using a lag of 5 points [10], and the specific values of the recurrence variables were determined. The process was repeated using points 2–31, which yielded the next values of the recurrence variables. Successively shifting the window forward by one point resulted in the recurrence time series $\%R(t)$ and $\%D(t)$. The changes induced in the EEG by the field were more easily detected by analyzing $\overline{\%R(t)}$ and $\overline{\%D(t)}$, smoothed versions of $\%R(t)$ and $\%D(t)$, respectively, produced by use of a sliding averaging window of 100 ms (see below).

To detect the EPs, $\%R(t)$ and $\overline{\%D(t)}$ were computed for each epoch of interest in $V(t)$ (Fig. 1d), namely $t = 0.1$–0.5, $t = 2.1$–2.5, and $t = 5.1$–5.5 s, respectively corresponding to the onset (EP_{on}), offset (EP_{off}), and control (EP_C) epochs (Fig. 1d), using a five-dimensional phase space and a time delay of 5 points (17 ms) [8]. The embedding and other analytical parameters were determined empirically in prior studies. All calculations were performed using publicly available software [11]; approximately 15% of the calculations were repeated using a custom Matlab code (Mathworks, Natick, MA, USA) to verify the accuracy of the results.

To synchronize the graphical representation of $V(t)$ and $\overline{\%R(t)}$, we adopted the convention that each point in $\overline{\%R(t)}$ was plotted at the time corresponding to the middle of the interval in $V(t)$ from which it was computed. For example, the value of $\%R(t)$ determined by the 100-ms interval in $V(t)$ beginning at $t = 100$ ms (RA window) would appear in a plot of $\%R(t)$ at $t = 150$ ms; when that point was the first point in the 100-ms averaging window for $\overline{\%R(t)}$, it was plotted at $t = 200$ ms. Thus, $\overline{\%R(200)}$ reflected determinism that occurred in $V(t)$ within 100–300 ms.

2.5. Linear analyses

As used here *evoked potentials* means any deterministic change in brain electrical activity caused by a stimulus (onset or offset of the field), whether or not the change was time-locked to the stimulus. To determine whether EPs could be detected by linear analysis of the EEG [12], $V(t)$ was analyzed directly (no embedding). In each trial, $V(t)$ was averaged over EP_{on}, EP_{off}, EP_C, E, and $C\left(V_{RMS} = \left[\sum_{i=1}^{60} V_i^2/300\right]^{1/2}\right)$, and the appropriate means were compared to test for field-induced linear effects. We planned to regard a change in brain electrical activity as nonlinear if it were detected in the recurrence time series but not in $V(t)$.

2.6. Experimental design and statistics

To detect the onset potentials we examined the 60 points in $\overline{\%R(t)}$ and in $\overline{\%D(t)}$ (0.2–0.4 s) which contained the dynamical activity in $V(t)$ at 0.1–0.5 s after field onset (EP_{on} epoch, Fig. 1d). Each of the 60 points was compared with its corresponding point in the control interval of the recurrence time series (5.2–5.4 s, which contained the determinism in EP_C) using the paired t-test at a pair-wise significance level of $p < 0.05$ (identical results were found using the Wilcoxon signed rank test). The offset evoked potential was detected by similarly comparing the determinism from EP_{off} with that from EP_C.

In preliminary studies involving baseline EEG (no field), we compared 2048 sets of 50 sham-field versus control comparisons, and found that the probability of observing ≥10 significant tests (out of 60, in succession) in a recurrence time series due to chance was about 0.04. Therefore, as previously [6], we regarded a comparison of a set of evoked potential and control epochs from any particular electrode as significant if ≥10 tests were pair-wise significant at $p < 0.05$.

Filtering the EEG in the alpha band facilitates detection of MEPs; sometimes filtering 9–12 Hz but not 8–10 Hz was effective, and sometimes conversely [6,13,14]. Sometimes both $\overline{\%R}$ and $\overline{\%D}$ revealed a field-induced change in the EEG, but sometimes only one or the other did so [14]. Based on these prior observations, we systematically considered all conditions of analysis previously shown capable of revealing a magnetosensory EP [14]. First, we analyzed $\overline{\%R(t)}$ in all 6 electrodes. If we found an evoked potential (≥10 pair-wise significant tests within the expected latency interval) in at least 3 electrodes, no further analyses were conducted. If fewer than 3 evoked potentials were found, we analyzed $\overline{\%D(t)}$. If a total of 3 evoked potentials were still not detected, we filtered $V(t)$ prior to calculating $\overline{\%R(t)}$ and $\overline{\%D(t)}$ and continued the analysis until either 3 evoked potentials were detected or all the 6 predetermined conditions (combinations of recurrence variable and filtering conditions) were considered. The overall results did not depend on the order; for presentation, we chose the sequence $\overline{\%R(t)}$, $\overline{\%D(t)}$, $\overline{\%R(t)}$ after filtering the EEG at 8–10 Hz, $\overline{\%D(t)}$ after filtering at 8–10 Hz, $\overline{\%R(t)}$ after filtering at 9–12 Hz, $\overline{\%D(t)}$ after filtering at 9–12 Hz.

To ensure the statistical reliability of the results, we calculated the family-wise error for each subject as follows. Whenever tests were done to compare the determinism in the EP_{on} and EP_C epochs, or EP_{off} and EP_C epochs, comparable comparisons were made using the sham data (sham evoked potential versus sham control). Thus, for example, when the experimental data was filtered at 8–10 Hz,

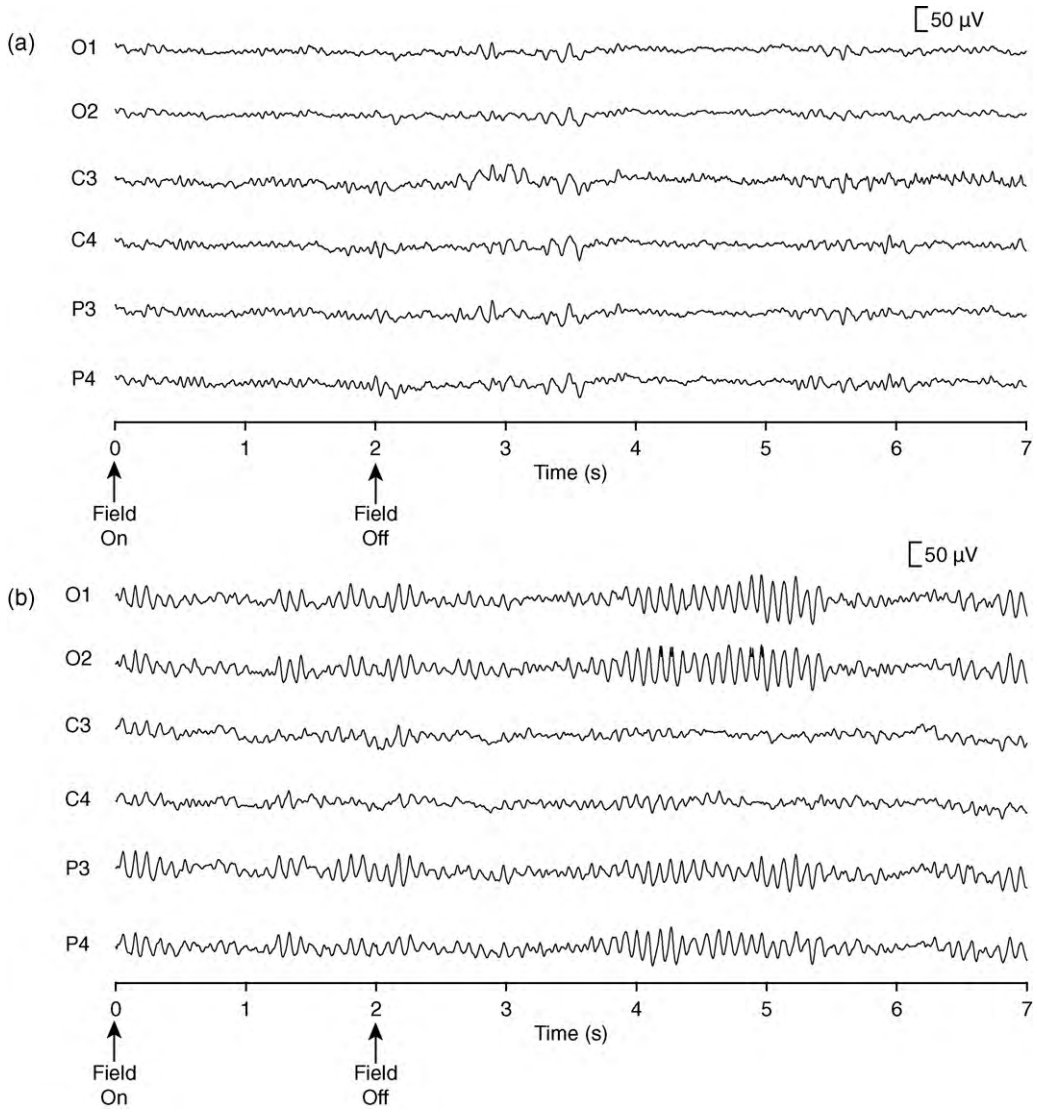

Fig. 2. Typical electroencephalograms in subjects exposed to 5 μT for the indicated duration. The signals were not digitally filtered. Neither transient nor steady-state induction artifacts appeared in the signals recorded from subjects with either low (a) or high (b) alpha power. Randomly selected trials from subject S1 (a) and S6 (b).

so was the sham data. At the conclusion of the study we calculated the *a posteriori* false-positive rate (number of false-positive effects in the sham data divided by the total number of tests performed), and used that error rate to estimate the family-wise error (P_{FW}) for the decision that the magnetic field had altered the subject's brain electrical activity.

Prior to the study we were unaware of whether the probability of detection of evoked potentials depended on the electrode derivation. We therefore computed the contributions to P_{FW} separately for the central, occipital, and parietal electrodes using the binomial formula, and the overall family-wise error rate for the effect in each experiment was determined by the law of compound probability.

3. 3. Results

3.1. Evoked potentials

Neither 5 nor 1 μT resulted in either transient or steady-state inductive artifacts in the EEG, regardless of whether the alpha power was low or high (Fig. 2a and b, respectively).

Using the nonlinear variable $\overline{\%R(t)}$, brain potentials evoked by field onset or offset were detected in 91% of the subjects (20/22) at 5 μT and in 73% of the subjects at 1 μT (16/22) (Tables 1 and 2, first data columns). Typical results are given in Fig. 3, which shows the offset potentials observed in subject S2 following termination of exposure to 1 μT. When $\overline{\%R(t)}$ was used to compare the EP_{off} and EP_C epochs (2.2–2.4 and 5.2–5.4 s, respectively) point-by-point, an evoked potential (>10 pair-wise significant tests) having the expected latency was detected from O1, O2, and P3 (Fig. 3, left panels); sham-field exposure (the negative control procedure) yielded no false-positive results (<10 significant tests in each derivation) (Fig. 3, right panels). A total of 2 stimuli × 6 derivations × 22 subjects = 264 statistical tests involving the $\overline{\%R(t)}$ time series were performed at 5 μT and at 1 μT resulting in 39 EPs at each field. At least one potential was detected in every subject (Tables 1 and 2, first data column).

When a subject exhibited fewer than 3 evoked potentials in response to either the onset or offset of the field, $\overline{\%D(t)}$ was computed and analyzed, and EPs were found that had not been detected with $\overline{\%R(t)}$ (Tables 1 and 2, second data column). At 5 μT, additional onset potentials were found in S3 and S13, and additional offset potentials were found in S17 (Table 1). At 1 μT the additional onset potentials occurred in S5 and S13, and additional offset potentials occurred in S1, S8, S15, and S22. Filtering the EEG to remove 8–10 Hz

Table 1
Evoked potentials in subjects (age, gender) exposed to 5 μT, 60 Hz. Column heads indicate conditions of analysis. Effects in $\overline{\%D(t)}$ are shown in bold. X, evoked potentials not detected. Bars indicate conditions not analyzed. P_{FW}, family-wise error for the decision that the subject exhibited evoked potentials. NE, no effect. False-positive detection results were found in the sham data for S7 (offset), S9 (offset), and S20 (offset).

Subject	MEP	$\overline{\%R}$	$\overline{\%D}$	$\overline{\%R}$ (8–10 Hz)	$\overline{\%D}$ (8–10 Hz)	$\overline{\%R}$ (9–12 Hz)	$\overline{\%D}$ (9–12 Hz)	All effects	No. tests	P_{FW}
S1 (52 F)	Onset	X	**X**	C4	O2 P4	—	—	**O2** C4 **P4**	24	0.016
	Offset	P4	X	C3	**C3**	—	—	C3 **C3** P4	23	0.018
S2 (58 F)	Onset	C3	X	P3	**C3**	—	—	C3 **C3** P3	23	0.018
	Offset	O1 O2	**O2**	—	—	—	—	O1 O2 **O2**	12	0.008
S3 (61 M)	Onset	C3	**O2 C3**	—	—	—	—	**O2** C3 **C3**	12	0.003
	Offset	C3 P3	**C3 P3**	—	—	—	—	C3 **C3** P3 **P3**	12	0.000
S4 (47 M)	Onset	X	X	O1	X	O2	**O1 O2**	O1 **O1** O2 **O2**	35	0.035
	Offset	X	X	O1	X	O2	**O1 O2**	O1 **O1** O2 **O2**	35	0.038
S5 (32 F)	Onset	O2 P3	**O2**	—	—	—	—	O2 **O2** P3	12	0.003
	Offset	X	X	X	X	X	**X**	X	36	NE
S6 (50 M)	Onset	X	X	X	X	X	X	X	36	NE
	Offset	P3	**P3**	X	X	P4	—	P3 **P3** P4	27	0.070
S7 (32 F)	Onset	P4	**P4**	X	**C4**	—	—	**C4** P4 **P4**	22	0.015
	Offset	X	X	X	X	X	X	X	36	NE
S8 (36 F)	Onset	O2	X	X	X	P4	X	O2 P4	34	NE
	Offset	O2	**O2**	C4	—	—	—	O2 **O2** C4	17	0.008
S9 (47 F)	Onset	X	X	X	X	C4	X	C4	36	NE
	Offset	O2	**O2**	X	X	C4	—	O2 **O2** C4	27	0.025
S10 (40 M)	Onset	O2 P4	**O2 P4**	X	—	—	—	O2 **O2** P4 **P4**	12	0.000
	Offset	X	X		**P4**	X	X	P4	35	NE
S11 (41 M)	Onset	C3	**C3**	P3	—	—	—	C3 **C3** P3	17	0.008
	Offset	O1 O2 C3 P3	—	—	—	—	—	O1 O2 C3 P3	6	0.000
S12 (26 M)	Onset	X	X	X	X	X	**X**	X	36	NE
	Offset	O1	**O1**	C3 P3 P4	—	—	—	O1 **O1** C3 P3 P4	17	0.000
S13 (29 M)	Onset	C4 P4	**C4 P3 P4**	—	—	—	—	C4 **C4 P3** P4 **P4**	12	0.000
	Offset	X	X	X	X	X	**O1**	**O1**	36	NE
S14 (31 F)	Onset	X	X	C3	**C3**	X	**X**	C3 **C3**	34	NE
	Offset	O1 P3	**O1 P3**	—	—	—	—	O1 **O1** P3 **P3**	12	0.000
S15 (23 M)	Onset	O1 C3	**O1 C3**	—	—	—	—	O1 **O1** C3 **C3**	12	0.000
	Offset	O1 C4	**O1 C4**	—	—	—	—	O1 **O1** C4 **C4**	12	0.000
S16 (22 F)	Onset	X	X	O2 C3 C4	—	—	—	O2 C3 C4	18	0.010
	Offset	C3	**C3**	X	X	X	X	C3 **C3**	32	NE
S17 (23 F)	Onset	O1	**O1**	X	X	X	X	O1 **O1**	32	NE
	Offset	X	**O1**	C4 P4	—	—	—	**O1** C4 P4	18	0.008
S18 (23 M)	Onset	P4	**P4**	X	X	C3	—	C3 P4 **P4**	27	0.025
	Offset	C4 P4	**C4**	—	—	—	—	C4 **C4** P4	12	0.003
S19 (26 M)	Onset	O1	**O1**	X	X	X	X	O1 **O1**	32	NE
	Offset	C4	**C4**	O2 P3	—	—	—	O2 C4 **C4** P3	17	0.001
S20 (49 F)	Onset	O1	X	C4	**C4 P4**	—	—	O1 C4 **C4 P4**	23	0.002
	Offset	X	X	X	X	X	**C4**	**C4**	36	NE
S21 (28 F)	Onset	X	X	X	X	X	X	X	36	NE
	Offset	X	X	X	**C3**	—	—	**C3**	35	NE
S22 (27 F)	Onset	P3	X	X	X	X	X	P3	34	NE
	Offset	X	X	X	X	X	X	X	36	NE

or 9–12 Hz prior to computing $\overline{\%R(t)}$ or $\overline{\%D(t)}$ revealed additional potentials. For example, at 5 μT, when the 8–10-Hz energy was removed from the EEG signals prior to computing $\overline{\%R(t)}$, previously undetected potentials were found in 11 subjects (S1, S2, S4, S8, S11, S12, S14, S16, S17, S19, and S20); at 1 μT additional potentials were found in 11 subjects (S3, S5, S6, S8, S11, S13–S16, S18, and S22). Based on our rule involving three detected effects, every subject detected 5 μT except S21 and S22, and every subject detected 1 μT except S3, S9, S17, S18, and S20 (Tables 1 and 2).

A total of 2132 tests were done in the sham data, and they resulted in 76 false-positive results. The corresponding pair-wise error rate (76/2132 = 0.0356) was used to compute P_{FW}, the *a posteriori* family-wise error rate for the decision that the stimulus had been transduced. Overall, there were 8 false-positive results (Tables 1 and 2).

Neither the latency nor duration of the potentials depended on the stimulus (onset or offset), stimulus strength, gender, or electrode derivation (Table 3). When the recurrence variable for each evoked potential (Tables 1 and 2) was compared with its control (expressed as a percent of the average of the sum), the change was sometimes greater than the control (37 ± 18%), and sometimes less (32 ± 14%) (Fig. 4).

Evoked potentials were not detected in any subject based on an analysis of the EEG using time averaging. Typical results are shown

Table 2
Evoked potentials in subjects exposed to 1 μT. Column heads indicate conditions of analysis. Effects in $\overline{\%D(t)}$ are shown in bold. X, evoked potentials not detected. Bars indicate conditions not analyzed. P_{FW}, family-wise error for the decision that the subject exhibited evoked potentials. NE, no effect. False-positive results were found in the sham data for S8 (onset), S9 (offset), S11 (onset), S20 (onset), and S22 (onset).

Subject	MEP	$\overline{\%R}$	$\overline{\%D}$	$\overline{\%R}$ (8–10 Hz)	$\overline{\%D}$ (8–10 Hz)	$\overline{\%R}$ (9–12 Hz)	$\overline{\%D}$ (9–12 Hz)	All effects	No. tests	P_{FW}
S1 (52 F)	Onset	X	X	X	X	X	**C4**	C4	36	NE
	Offset	O2	**O1**	O1	—	—	—	O1 **O1** O2	17	0.021
S2 (58 F)	Onset	X	X	X	X	X	X	X	36	NE
	Offset	O1 O2 P3	—	—	—	—	—	O1 O2 P3	6	0.000
S3 (61 M)	Onset	X	X	X	X	O2	**P3**	O2 **P3**	36	NE
	Offset	X	X	P3	**P3**	X	X	P3 **P3**	34	NE
S4 (47 M)	Onset	X	X	X	X	C3 P3	**C3**	C3 **C3** P3	36	0.056
	Offset	O1 O2 C3 C4 P3 P4	—	—	—	—	—	O1 O2 C3 C4 P3 P4	6	0.000
S5 (32 F)	Onset	X	**P4**	X	X	O2	X	O2 **P4**	34	NE
	Offset	P4	X	C4	**C4**	—	—	C4 **C4** P4	23	0.019
S6 (50 M)	Onset	X	X	X	X	X	X	X	36	NE
	Offset	C4	**C4**	C3 P4	—	—	—	C3 C4 **C4** P4	17	0.001
S7 (32 F)	Onset	C3 C4	**C3**	—	—	—	—	C3 **C3** C4	12	0.008
	Offset	C3 C4 P3	—	—	—	—	—	C3 C4 P3	6	0.000
S8 (36 F)	Onset	X	X	P4	**O2 C4 P4**	—	—	**O2 C4** P4 **P4**	24	0.002
	Offset	X	**O1 P3**	P4	—	—	—	**O1 P3** P4	18	0.010
S9 (47 F)	Onset	O1	X	X	X	X	X	O1	34	NE
	Offset	O1	X	X	X	X	X	O1	34	NE
S10 (40 M)	Onset	O1 P3	**P3**	—	—	—	—	O1 P3 **P3**	12	0.003
	Offset	P3	**P3**	X	X	X	X	**P3** P3	32	NE
S11 (41 M)	Onset	X	X	X	X	C4 P4	X	C4 P4	36	NE
	Offset	X	X	C4	**C4**	O1 O2	—	O1 O2 C4 **C4**	29	0.007
S12 (26 M)	Onset	C4 P3	**C4 P3**	—	—	—	—	C4 **C4** P3 **P3**	12	0.000
	Offset	O2	**O2**	X	X	X	X	O2 **O2**	32	NE
S13 (29 M)	Onset	X	**P4**	C4	**C4 P4**	—	—	C4 **C4 P4 P4**	23	0.003
	Offset	X	X	X	X	X	X	X	36	NE
S14 (31 F)	Onset	X	X	C3	**C3 C4**	—	—	C3 **C3 C4**	24	0.016
	Offset	X	X	O1	X	X	X	O1	35	NE
S15 (23 M)	Onset	O2 P4	**O2 P4**	—	—	—	—	O2 **O2** P4 **P4**	12	0.000
	Offset	O2	**P4**	C4 P4	—	—	—	O2 C4 P4 **P4**	17	0.001
S16 (22 F)	Onset	X	X	C3	X	C4 P3	—	C3 C4 P3	29	0.032
	Offset	C3	X	X	X	X	X	C3	34	NE
S17 (23 F)	Onset	X	X	X	X	C4	**C4**	C4 **C4**		NE
	Offset	C3	**C3**	X	X	X	X	C3 **C3**	32	NE
S18 (23 M)	Onset	X	X	P3	**P4**	X	X	P3 **P4**	34	NE
	Offset	X	X	X	X	X	X	X	36	NE
S19 (26 M)	Onset	C4 P4	**C4 P4**	—	—	—	—	C4 **C4** P4 **P4**	12	0.000
	Offset	C4	X	X	X	X	X	C4	34	NE
S20 (49 F)	Onset	X	X	X	X	X	**O1**	O1	36	NE
	Offset	O2	**O2**	X	X	X	**X**	**O2** O2	32	NE
S21 (28 F)	Onset	C3 P3	**C3 P3**	—	—	—	—	C3 **C3** P3 **P3**	12	0.000
	Offset	P3	**P3**	X	X	O1 O2	—	O1 O2 P3 **P3**	27	0.005
S22 (27 F)	Onset	X	X	C3 P3	**C3 P3**	—	—	C3 **C3** P3 **P3**	24	0.003
	Offset	O2 P3	**O1 O2 C3 P3**	—	—	—	—	**O1** O2 **O2 C3** P3 **P3**	12	0.000

Table 3
Latency and duration of evoked potentials stratified by stimulus (onset or offset), gender, and electrode derivation (neither parameter depended on field strength). Mean ± SD. *N*, number of evoked potentials (from Tables 1 and 2).

	Stimulus		Gender		Electrode		
	Onset	Offset	Male	Female	Occipital	Central	Parietal
Latency (ms)	306 ± 49	304 ± 55	301 ± 51	308 ± 53	300 ± 54	305 ± 50	310 ± 53
Duration (ms)	267 ± 31	266 ± 29	270 ± 32	265 ± 28	268 ± 30	264 ± 23	267 ± 35
N	110	113	113	110	70	81	72

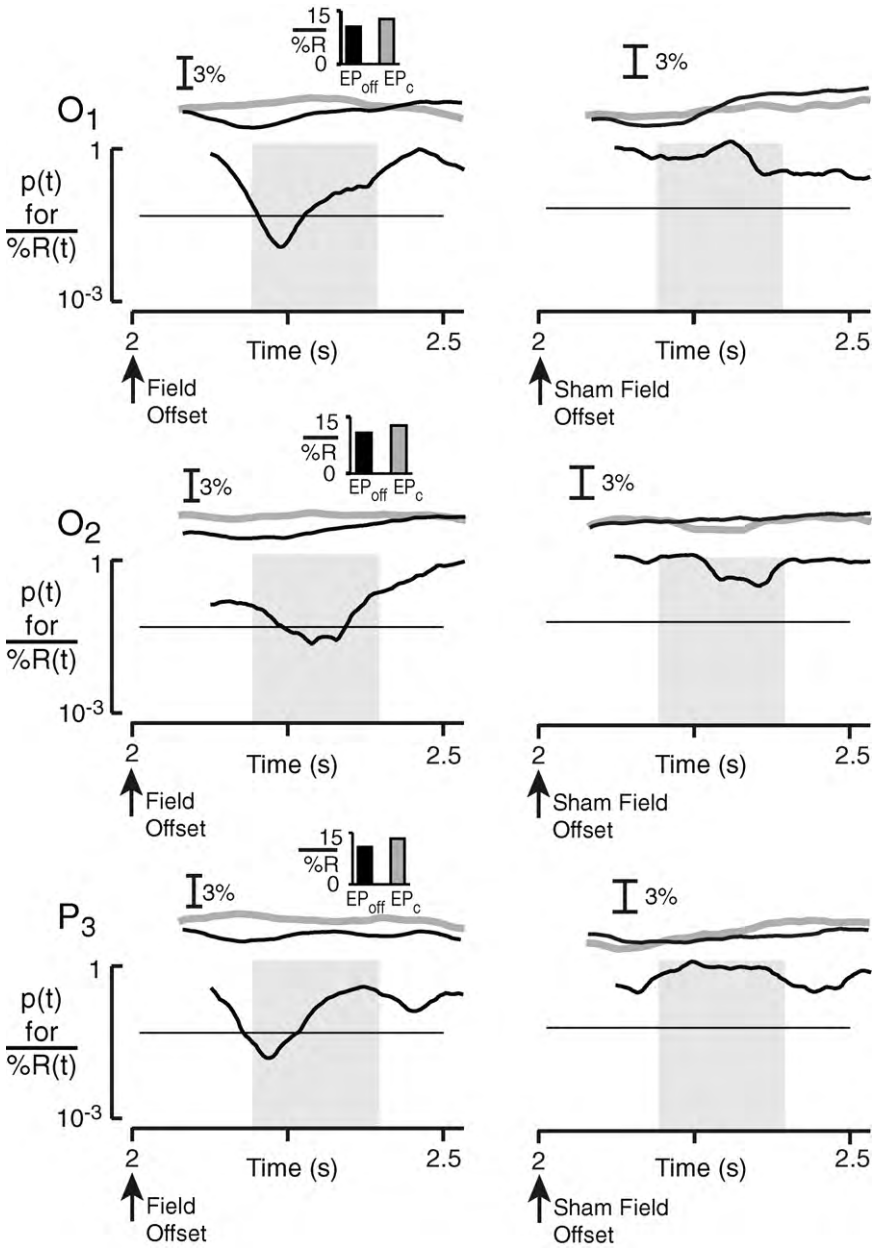

Fig. 3. Offset evoked potentials from 3 derivations in subject S2 triggered by termination of exposure to 1 μT, detected using the recurrence-plot analysis variable $\overline{\%R(t)}$. Exposure and sham-exposure results are shown in the left and right panels, respectively. The curves at the tops of the panels show the average values of $\overline{\%R(t)}$ during $t = 2.03–3$ s and $t = 5.03–6$ s (intervals that contained EP_{off} and EP_C in the $\overline{\%R}$ time series) ($N \geq 50$ trials). The $p(t)$ curves are the probability that the difference between the means of the offset and control curves at time t was due to chance. Bar graphs indicate the average value of $\overline{\%R}$ over the latency interval for which $p(t) < 0.05$ (horizontal line); the standard deviations are not resolved at scale shown. The stippled regions show the expected $\overline{\%R(t)}$ latency intervals (2.2–2.4 s). The ordinates are shown on a log scale.

in Fig. 5. Neither time averaging of the EEG nor point-by-point comparisons (Fig. 5a and b, left column) provided any evidence of evoked potentials. In contrast, evoked potentials were detected by means of recurrence-plot analysis (Fig. 5a and b, right column).

4. Discussion

Epidemiological studies suggested that power-frequency EMFs in the environment have serious public-health implications [15]. Knowledge of the physiological process that mediates the putative link between fields and disease would significantly improve our ability to interpret the epidemiological studies. Stress is one possible mediative process, and electrophysiological [6], endocrinological [2], and immunological [3,4] evidence has been adduced in support of the stressor hypothesis. Nevertheless the critically important evidence that environmental fields can be detected has not yet been provided. We applied spatially and spectrally well-controlled fields of 1 and 5 μT under conditions that permitted independent determinations of whether either field triggered onset or offset EPs. We planned to interpret the EPs as support for the stressor theory to the extent that they would evidence sensory transduction, the earliest step in the stress response.

Onset potentials were seen in all but 3 subjects (S6, S9, and S17) and offset potentials were seen in all but 4 subjects (S10, S13, S16, and S20) (Tables 1 and 2); every subject exhibited an onset and/or offset EP. Several considerations indicated that the effects were true evoked potentials. First, the analysis incorporated protection against family-wise error, which obviated an explanation based on chance. Second, comparable changes were not observed in the sham data. Third, the changes occurred several hundred millisec-

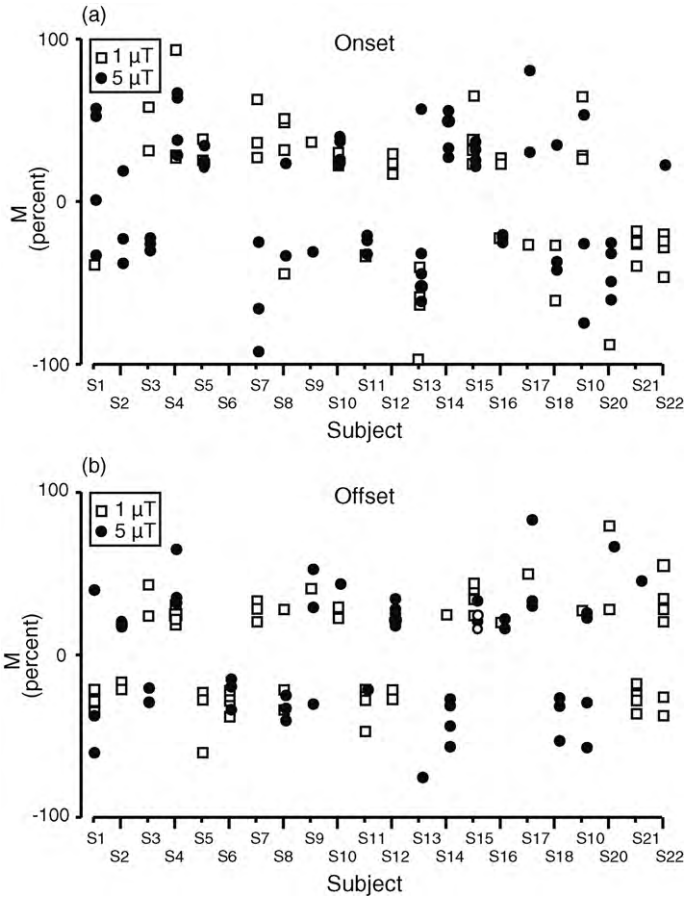

Fig. 4. Relative magnitude (M) of each evoked potential (expressed in percent) from each subject as determined by recurrence analysis. (a) and (b) Onset and offset responses, respectively. For each potential, $M = 100(E - C)/0.5(E + C)$, where E was the average of the recurrence variable over the statistically significant latency interval, and C was the corresponding average in the control epoch. Where necessary, points were jittered to facilitate resolution. Values greater than 100% are shown as 100%.

onds after the field had been switched off, which was consistent with the inference that the changes arose from brain processing of afferent signals that resulted from transduction of the field. The observed latency was inconsistent with the possibility that the changes could have been generated by a field-electrode interaction because that process has no latency. Fourth, studies using phantoms of the human head verified the absence of electrode signals within the expected latency range.

Filtering within the alpha band was sometimes necessary for detection of the evoked potentials (Table 1), as observed previously [6,13,14]. The amount of alpha power, the levels of which are generally associated with alertness [16], varied from subject to subject (Fig. 2), and could not be controlled directly. The rationale for removing alpha energy was that it did not contribute to the response, and therefore that removal of alpha increased sensitivity for detection of the EPs by increasing the signal-to-noise ratio in the system. The increased sensitivity afforded by alpha filtering might mean that the brain region where the alpha activities originate, usually assumed to be the cerebral cortex [16], was not crucial in the brain processing that gave rise to the EPs. Alternatively, the increased sensitivity afforded by alpha filtering might be related to differences among the subjects in their level of alertness during the experimental session.

The evoked potentials were not detected when the EEGs were analyzed by time averaging, indicating that they were not time-locked but rather nonlinear in origin, as observed previously [6,13,14]. The finding that the changes in recurrence parameters could be either an increase or a decrease (Fig. 4) further confirmed the nonlinearity of the response, because (1) it is characteristic behavior of a nonlinear system, and (2) only nonlinear systems can exhibit such behavior.

The effects (Tables 1 and 2) were robust, as evidenced by our ability to detect them in almost all of the subjects, and by the magnitude of the effects. For example, the average change in the nonlinear variables used to characterize the EPs was greater than 30% (Fig. 4). Clinical EPs, in contrast, typically exhibit an average rms change in $V(t)$ of less than 10% [17].

Why were the evoked potentials nonlinear? One possibility is that the sensory system which produced them has no evolutionary purpose. It is reasonable to view the processes responsible for the linear correspondence between the common stimuli and the responses they induce as resulting from evolution by natural selection, leading progressively to physiological systems that conferred a selective advantage because they were reliable. Conversely, in the absence of natural selection there is no process by which the phenomenon of consistency in response to a stimulus can come about. Power-frequency fields were negligible throughout the period of evolution of life on earth and became a prominent part of the environment only within the last century. They could not have served as an agent of evolutionary change, and consequently, a physical mechanism capable of producing a predictable response (a dose-related response that reliably occurs in the same direction) to fields did not develop. In this view, one possible explanation for the existence of a nonlinear human magnetic sense could be that it arose as a vulnerability in the molecular machinery chosen by evolution to mediate other sensory modalities [18]. Any physical realization of a sensory system for one kind of stimulus is unlikely to be completely immune to all other kinds of inputs. Magnetic phosphenes [19] and microwave hearing [20] are two examples of nonfunctional (from an evolutionary standpoint) sensory responsiveness. Electric and magnetic receptors that facilitate finding food, avoiding predators, and navigating in the environment occur in various life forms [21–25]. Such functional structures have not been reported in human beings, but vestiges of parts of these detection systems might still exist in human beings.

We did not address the question of the anatomical location of the electroreceptor cell. Although the observed latencies (Table 3) were consistent with the electroreceptor cell being located anywhere in the body, animal studies suggested that the detecting cell was located in the head [26]. In rats, glucose utilization was specifically increased in the hindbrain, as assessed by positron emission tomography [27], but the result may mean that early post-transduction processing (rather than transduction itself) occurred in the hindbrain. The field-induced effects on the EEG were approximately equally likely to occur in any of the electrodes (Table 3), perhaps indicating that none of the electrodes was especially close to the detection site.

We also did not address the question of the biophysical basis of the detection process. However we previously presented evidence that the coupling between environmental EMFs and brain tissue was mediated by negatively charged oligosaccharide side chains bound to the gate of an ion channel whose gating characteristics were affected by the electric field induced in the tissue by the magnetic component of the environmental EMF [28].

A review of reports describing measurements of environmental power-frequency magnetic fields confirmed that the field strengths used in our experiments were directly comparable to the power-frequency fields in work and home environments. Averaged over the workday, non-flying airline workers were exposed to 0.04–0.2 μT (measured at the waist), depending on job category [29]. Approximately 36% of children in a study of the link between magnetic-field exposure and acute lymphoblastic leukemia expe-

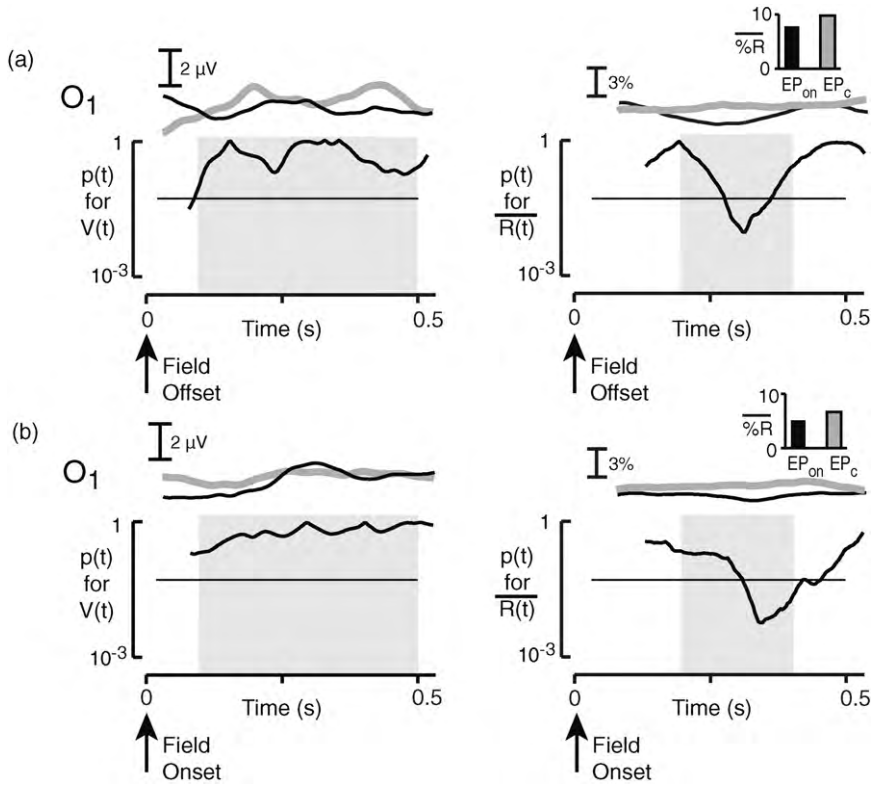

Fig. 5. Linear and nonlinear analysis of evoked potentials. First column, effect of stimulus assessed by time averaging, using $V(t)$. Second column, effect assessed using $\overline{\%R(t)}$ computed from $V(t)$. (a) EEG from O1 in subject S11 (5 μT) for the time interval following field offset. (b) EEG from O1 in subject S19 (5 μT) for the time interval following field onset. The curves at the tops of the panels show the average values of the time series for the intervals that contained EP_{off} and EP_C ($N \geq 50$ trials). The $p(t)$ curves are the probability that the difference in means at time t was due to chance. Bar graphs indicate the average value of $\overline{\%R}$ over the latency interval for which $p(t) < 0.05$ (horizontal line); the standard deviations are not resolved at scale shown. The stippled regions show the expected latency interval (0.1–0.5 s in $V(t)$, 0.2–0.4 s in $\overline{\%R(t)}$). The ordinates are shown on a log scale.

rienced fields greater than 1 μT [30]. The average field exposure for workers in 5 electrical job categories was 2.3 μT [31]. A typical electric power substation in an urban environment had a field greater than 2 μT along half of its perimeter, and a field between 0.2 and 2 μT along the other half [32]. In a sample of 1000 homes, about 5% had an average field of 0.3 μT [33]. In a group of 100 pregnant women, 23% experienced at least one exposure greater than 2 μT during a 7-day period [34]. The fetus in a woman passing through a metal detector experiences an average magnetic field of about 10 μT (1000 Hz) [35]. In Modena and Reggio Emilia, the average exposure of workers representative of the main occupations was 0.6 μT [36]. The female work force in Stockholm spent about 23% of their workday exposed to greater than 0.3 μT [37]. In Taiwan, pharmacists and their assistants were exposed to magnetic fields that varied between 0.05 and 2 μT depending on location within their work environment; the time-weighted average over the workday was 0.5–0.8 μT [38]. In Seoul, field exposure averaged over 24 h was 0.08–0.8 μT in a study population of more than 100 subjects [39]. Considered as a group, the studies established that the field strengths we employed were common in the environment.

In summary, 1–5 μT, 60 Hz, produced changes in brain electrical activity indicative of a detection process based on sensory transduction. These results, taken together with the environmental measurements [29–39], implied that brain activity in a substantial portion of the population, worldwide, is more or less continuously affected as a side-effect of the commercial electric power generation and distribution systems. The results also implied that environmental fields were detected by means of sensory transduction, like other stressors. To that extent the results supported the stressor theory linking field exposure and disease because they explained how environmental energy could be converted into a biological signal. Nevertheless the results do not directly show that all or even some long-term exposure results in disease, because not all biological signals lead to disease. With regard to disease causation, we think that the implications of our results are limited to warranting further exploration of the public-health consequences of EMF exposure, especially the consideration of studies involving multiple simultaneous EMFs, which is the common condition in the environment.

Conflict of interest

The authors have no financial or personal relationships with other people or organizations that could inappropriately influence or bias their work.

References

[1] Becker RO, Marino AA. Electromagnetism & life. Albany: State University of New York Press; 1982.
[2] Marino AA. Electromagnetic fields, cancer, and the theory of neuroendocrine-related promotion. Bioelectrochem Bioenerg 1993;29:255–76.
[3] Marino AA, Wolcott RM, Chervenak R, Jourd'heuil F, Nilsen E, Frilot C. Nonlinear response of the immune system to power-frequency magnetic fields. Am J Physiol Regul Integrative Comp Physiol 2000;279:R761–8.
[4] Marino AA, Wolcott RM, Chervenak R, Jourd'heuil F, Nilsen E, Frilot II C. Nonlinear determinism in the immune system. In vivo influence of electromagnetic fields on different fucntions of murine lymphocyte subpopulations. Immunol Invest 2001;30:313–34.
[5] Zbilut JP, Webber Jr CL. Recurrence quantification analysis. In: Akay M, editor. Wiley encyclopedia of biomedical engineering. Hoboken: John Wiley & Sons; 2006. p. 2979–86.
[6] Carrubba S, Frilot C, Chesson Jr AL, Marino AA. Evidence of a nonlinear human magnetic sense. Neuroscience 2007;144:356–67.
[7] Klem GH. Artifacts. In: Ebersole JS, Pedley TA, editors. Current practice of clinical electroencephalography. Philadelphia: Lippincott Williams & Wilkins; 2003. p. 271–87.

[8] Carrubba S, Frilot C, Chesson A, Marino A. Detection of nonlinear event-related potentials. J Neurosci Meth 2006;157:39–47.
[9] Takens F. Detecting strange attractors in turbulence. Dynamical systems and turbulence. Berlin: Springer; 1981.
[10] Eckmann J-P, Kamphorst SO, Ruelle D. Recurrence plots of dynamical systems. Europhys Lett 1987;4:973–9.
[11] Webber CL, Jr. Recurrence quantification analysis. http://homepages.luc.edu/~cwebber. 2007. Accessed June 30, 2009.
[12] Ruchkin DS. Measurement of event-related potentials: signal extraction. In: Picton TW, editor. Human event-related potentials, handbook of electroencephalography and clinical neurophysiology. New York: Elsevier; 1988.
[13] Carrubba S, Frilot C, Chesson Jr AL, Marino AA. Nonlinear EEG activation by low-strength low-frequency magnetic fields. Neurosci Lett 2007;417:212–6.
[14] Carrubba S, Frilot C, Chesson Jr AL, Webber Jr CL, Zbilut JP, Marino AA. Magnetosensory evoked potentials: consistent nonlinear phenomena. Neurosci Res 2008;60:95–105.
[15] Hardell L, Holmberg B, Malker H, Paullson LE. Exposure to extremely low frequency electromagnetic fields and the risk of malignant diseases—an evaluation of epidemiological and experimental findings. Eur J Cancer Prev 1995;4(Suppl. 1):3–107.
[16] Shaw JC. The brain's alpha rhythms and the mind. Amsterdam: Elsevier; 2003.
[17] Robinson K, Rudge P. Abnormalities of the auditory evoked potentials in patients with multiple sclerosis. Brain 1977;100(Pt 1):19–40.
[18] Nesse RM, Williams GC. Evolution and the origins of disease. Sci Am 1998;279:86–93.
[19] Antal A, Kincxes TZ, Nitsche MA. Manipulation of phosphene thresholds by transcranial direct current stimulation in man. Exp Brain Res 2003;150:375–8.
[20] Frey AH. Human auditory systems response to modulated electromagnetic energy. J Appl Physiol 1962;17:689–92.
[21] Manger PR, Calford MB, Pettigrew JD. Properties of electrosensory neurons in the cortex. Proc R Soc Lond B Biol Sci 1996;263:611–7.
[22] Manger PR, Pettigrew JD, Keast JR, Bauer A. Nerve terminals of mucous gland electroreceptors in the platypus (*Ornithorhynchus anatinus*). Proc Biol Sci 1995;260:13–9.
[23] Nemec P, Altmann J, Marhold S, Burda H, Oelschläger HHA. Neuroanatomy of magnetoreception: the superior colliculus involved in magnetic orientation in a mammal. Science 2001;294:366–8.
[24] Wachtel AW, Szamier RB. Special cutaneous receptor organs of fish. IV. Ampullary organs of the nonelectric catfish Kryptopterus. J Morphol 1969;128:291–308.
[25] Walker MM, Diebel CE, Haugh CV, Pankhurst PM, Montgomery JC, Green CR. Structure and function of the vertebrate magnetic sense. Nature 1997;390:371–6.
[26] Marino AA, Nilsen E, Frilot C. Localization of electroreceptive function in rabbits. Physiol Behav 2003;79:803–10.
[27] Frilot II C, Carrubba S, Marino AA. Magnetosensory function in rats: localization using positron emission tomography. Synapse 2009;63:421–8.
[28] Carrubba S, Frilot IIC, Hart FX, Chesson Jr AL, Marino AA. The electric field is a sufficient physical determinant of the human magnetic sense. Int J Radiat Biol 2009;85:622–32.
[29] Kaune WT. Study of occupational magnetic-field personal exposures of non-flying airline employees. Richland, WA: National Institute of Occupational Safeaty and Health; 1999.
[30] Linet MS, Hatch EE, Kleinerman RA, Robison LL, Kaune WT, Friedman DR, et al. Residential exposure to magnetic fields and acute lymphoblastic leukemia in children. N Eng J Med 1997;337:1–7.
[31] McDevitt JJ, Breysse PN, Bowman JD, Sassone DM. Comparison of extremely low frequency (ELF) magnetic field personal exposure monitors. J Exp Anal Environ Epidemiol 2002;12:1–8.
[32] Silva JM, Hooper C. Post-construction EMF measurements for the Trumbull substation. Shelton, CT: The United Illuminating Company; 2008.
[33] Syfers R. EMF and childhood leukemia. EPRI J 2006. Spring, 24–31.
[34] Savitz DA, Herring AH, Mezei G, Evenson KR, Terry Jr JW, Kavet R. Physical activity and magnetic field exposure in pregnancy. Epidemiology 2006;17:222–5.
[35] Wu D, Qiang R, Chen JY, Seidman S, Witters D, Kainz W. Possible overexposure of pregnant women to emissions from a walk through metal detector. Phys Med Biol 2007;52:5735–48.
[36] Scaringi M, Bravo G, Vandelli AM, Romanelli A, Besutti G, Ghersi R, et al. Personal exposure to ELF magnetic fields in workers engaged in various occupations (in Italian). G Ital Med Lav Ergon 2005;27:342–5.
[37] Forssén UM, Mezei G, Nise G, Feychting M. Occupational magnetic field exposure among women in Stockholm County, Sweden. Occup Environ Med 2004;61:594–602.
[38] Li CY, Lin RS, Wu CH, Sung FC. Occupational exposures of pharmacists and pharmaceutical assistants to 60 Hz magnetic fields. Ind Health 2000;38:413–9.
[39] Kim YS, Cho YS. Exposure of workers to extremely low frequency magnetic fields and electric appliances. J Occup Health 2001;43:141–9.